THERMOMECHANICAL FRACTURE ANALYSIS OF PERFORATED TUBE

Rastislav ĎURIŠ, Milan NAĎ, Tibor NÁNÁSI

Authors: ***Ing. Rastislav Ďuriš, PhD.***
doc. Ing. Milan Naď, PhD.
Ing. Tibor Nánási, CSc.
Workplace: ***Slovak University of Technology in Bratislava,***
Faculty of Materials Science and Technology in Trnava,
Institute of Production Systems and Applied Mechanics,
Department of Applied Mechanics
Address: ***Rázusova 2, 917 24 Trnava, Slovak Republic***
E-mail: ***rastislav.duris@stuba.sk, milan.nad@stuba.sk, tibor.nanasi@stuba.sk***

Abstract

The main goal of paper is a fracture analysis of the crack located in the wall of perforated protective tube. The 3-D FEM simulations on two models with differently oriented cracks of varying lengths in software ANSYS were performed. Influence of steady-state temperature field on the fracture parameters was also investigated.

Key words

ANSYS, fracture analysis, stress intensity factor, J-integral, finite element method

Introduction

Linear elastic fracture mechanics (LEFM) is the basic of highly simplified theory of fracture. It is applicable to elastic material except of the vanishigly small region at the crack tip (front) (4). The most widely used fracture parameters are: SIF (*K*), *J*-integral (*J*), elastic energy release rate (*G*) and crack tip opening displacement (*CTOD*).
Stress intensity factors *K* are the measure of the stress-field change within the vicinity of the crack tip (front) for three basic modes of fracture (opening, shearing and tearing). Stress intensity factor has a significant role in the linear-elastic fracture mechanics. It can be expressed by relation

$$K = \sigma \sqrt{\pi\, a}\; Y \qquad [1]$$

where σ is nominal stress, a is crack length and Y is a nondimensional corrective function depending on the size and geometry of the crack, structural component and type of loading, which is for standard geometries published in literature (1, 2). The SIF for Mode I is compared against the critical value K_{IC} to determine whether or not the crack will propagate. For direct calculation of *K* values in general objects, several crack tip local approaches have been developed. In the post-yield 2-D fracture mechanics (as well as for elastic fracture too) *J*-integral in (4) was introduced. It was found to characterize the stress and strain fields surrounding the crack tip with significant plasticity, and also to corellate with fracture toughness J_{IC} (criterion of initiation) experimental results. In the simple 2-D form *J* around the counterclockwise path Γ is given by

$$J = \int_{\Gamma} W\, dy - \int_{\Gamma} \sigma_{ij}\, n_j\, u_{i,j}\, ds \qquad j = 1, 2 \qquad [2]$$

The discretized form of the *J*-integral in ANSYS is given by

$$J = \sum_{ie=1}^{ne} \left[\sigma_{ij}\, u_{i,1} - W\, \delta_{1i} \right] w_i\, q_{,i}\, A_{ie} \qquad [3]$$

where w_i is the weight function, A_{ie} is the area of the element *ie*, *q* is the crack-extension vector, *W* is strain energy density, n_j is outward unit normal vector on integration path, u_i are displacements and σ_{ij} is stress tensor and *ne* is the number of elements to be integrated.

If the thermal strains occur in the structure and the surface tractions act on crack faces, the *J*-integral is expressed as

$$J = \int_A \left[\sigma_{ij}\, u_{i,1} - W\, \delta_{1i} \right] q_{,i}\, dA + \int_A \alpha\, \sigma_{ii}\, \Theta_{,1}\, q_1\, dA - \int_C T_i\, u_{j,1}\, q_1\, ds \qquad [4]$$

where α is the thermal expansion coefficient, T_i is the crack face traction, δ_{ij} is a Kronecker delta and *C* is crack face upon which the tractions act.

For the 2-D crack problem, the crack-tip node component usually contains one node which is also the crack-tip node. The first contour for the area integration of the *J*-integral is evaluated over the elements associated with the crack-tip node component. The second contour for the area integration of the *J*-integral is evaluated over the elements adjacent to the first contour of elements. This procedure is repeated for all contours. To ensure correct results, the elements for the contour integration should not reach the outer boundary of the model (with the exception of the crack surface) (6).

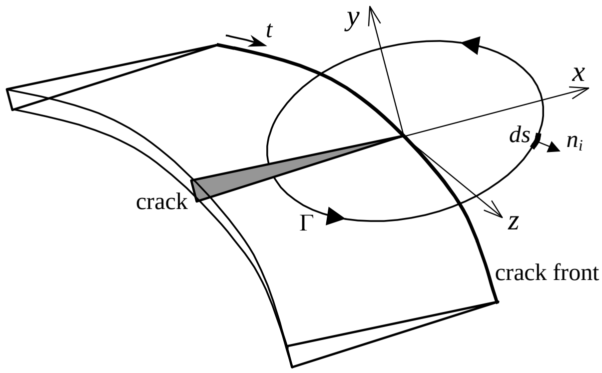

Fig. 1 *Definition of crack calculation parameters*

For the 3-D crack problem, the crack-tip node component is comprised of the nodes located along the crack front. For the 3-D problem, domain integral representation of the *J*-integral becomes a volume integration.

For 3-D problems, *J*-integral can be defined at any point of crack front by line integral along the path Γ and surface integral in the domain *A*(Γ) as is presented in (5)

$$J = \int_{\Gamma} (W\, n_k - T_i\, u_{i,k}) ds + \int_{A(\Gamma)} (W\, \delta_{k3} - \sigma_{i3}\, u_{i,k})_{,3}\, dA \qquad k = 1, 2, 3 \qquad [5]$$

Geometry, material properties and loading of models

For carrying out the analysis a problem of perforated protective tube with cracks across the wall thickness was chosen. The pipe geometry parameters are: outer pipe diameter D = 210mm, inner pipe diameter d = 178mm, lenght of pipe model L = 650mm, hole diameter D_{hole} = 32mm and wall thickness t = 16mm. The layout of holes in the tube wall can be seen in Fig. 2. Material of tube was 08CH18N10T with temperature dependent material parameters summarized in Table 1. During the nonstandard reactor operation, the different loading effects are acting on protective tubes, which may cause the unacceptable tube loadings. Both simulation models were loaded by the bending moment 6000Nm producing maximum bending stresses in the crack area. Equivalent stresses computed in the specimen were under the elastic limit (except a small area in the vicinity of the crack).

PIPE MATERIAL PROPERTIES Table 1

08CH18N10T								
T [°C]	20	50	100	150	200	250	300	350
$R_{p0,2}$ [MPa]	196	193	186	181	176	167	162	157
R_m [MPa]	490	477	456	426	417	382	358	333
E [GPa]	205	202	200	195	190	185	180	175
A_5 [%]	35	34	33	31	29	27	26	25

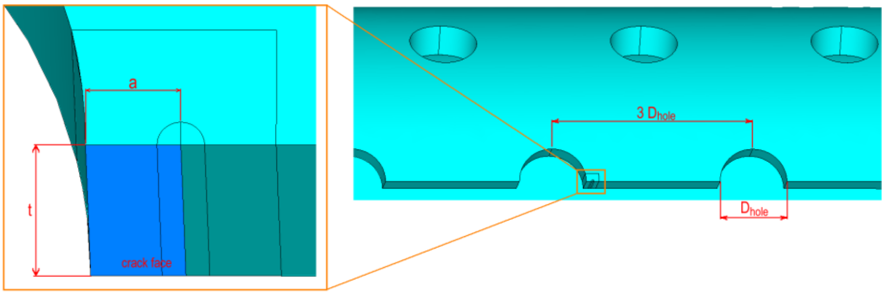

Fig. 2 *Geometry of tube and crack parameters*

In numerical analyses two locations and orientations of crack in thick-walled part of protective tube with various lenght of crack were considered (Fig. 3). Length of crack was chosen as a = (2; 3; 4; 5; 6; 8)mm in *Model 1* (longitudinal crack) and as a = (1; 2; 3; 4; 5, 6)mm in *Model 2* (perpendicular crack).

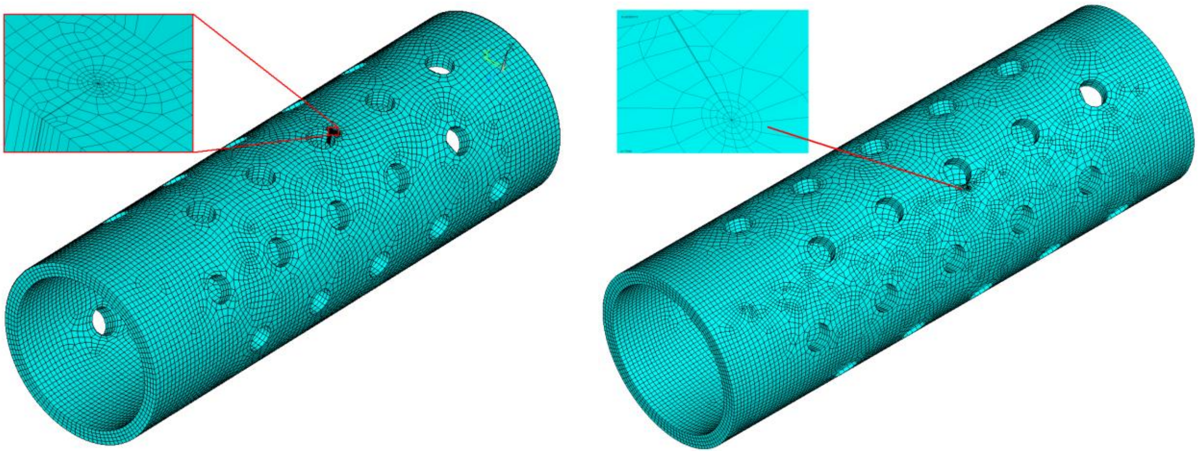

Model 1 ***Model 2***

Fig. 3 *Geometry of part of protective tube with detail of mesh in the crack front vicinity*

Numerical simulations

Numerical simulations were carried out using ANSYS FEM software. Loading of the model was chosen such that deformation of the short tube model is equal to 0,2% of the full length tube 4180 mm. Both models with different crack location were loaded without and/or with considering the effect of the temperature field in the tube. The steady-state temperature field caused by heating the tube up to 315 °C against the reference room temperature 20 °C was considered. Thermal expansion coefficient $\alpha = 1{,}2.10^{-5}K^{-1}$. For calculation of SIFs quarter-point (singular) elements near the crack front and KCALC command were used. Mesh with high-order SOLID finite elements and CINT macro were used for calculation of *J*-integral values.

Results of FE simulations

In Fig. 4 the results of calculation of K_I-factors at the outer tube diameter (0mm coordinate in thickness), inner tube diameter (16mm coordinate in thickness) and in the middle of tube wall (8mm coordinate in thicknees) for both models are presented. Maximum values of K_I-factor were identified on the outside of the tube with perpendicular crack (*Model 2*). In *Model 1* with longitudinal crack was maximum of K_I obtained at inner surface of the tube. Results of K_{II}- and K_{III}-factors calculation for the considered type of loading achieved values less than 1% of K_I and therefore are not presented here.
Graphs on the left present results of numerical analyses without influence of temperature. Graphs on the right of figures show results obtained when the steady-state temperature field in the tube is considered.

Model 1

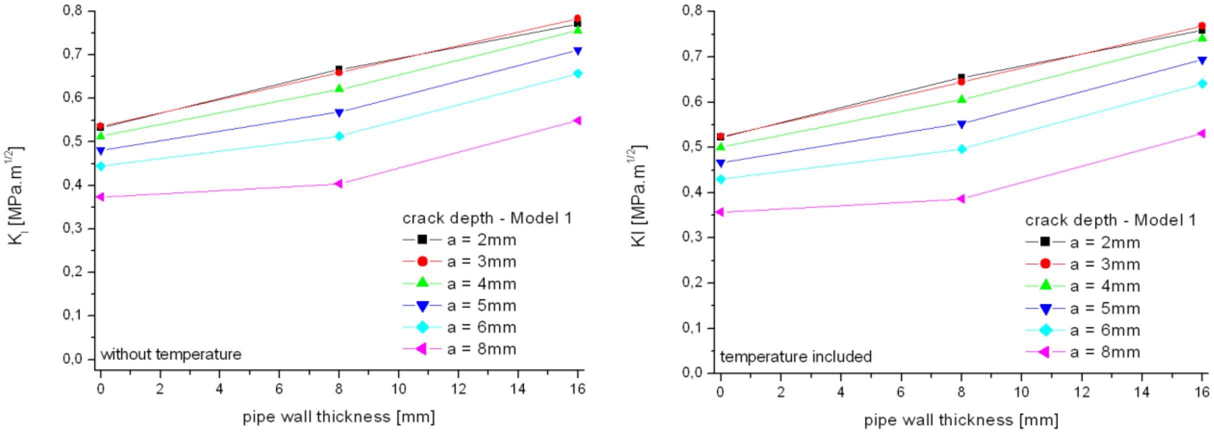

Model 2

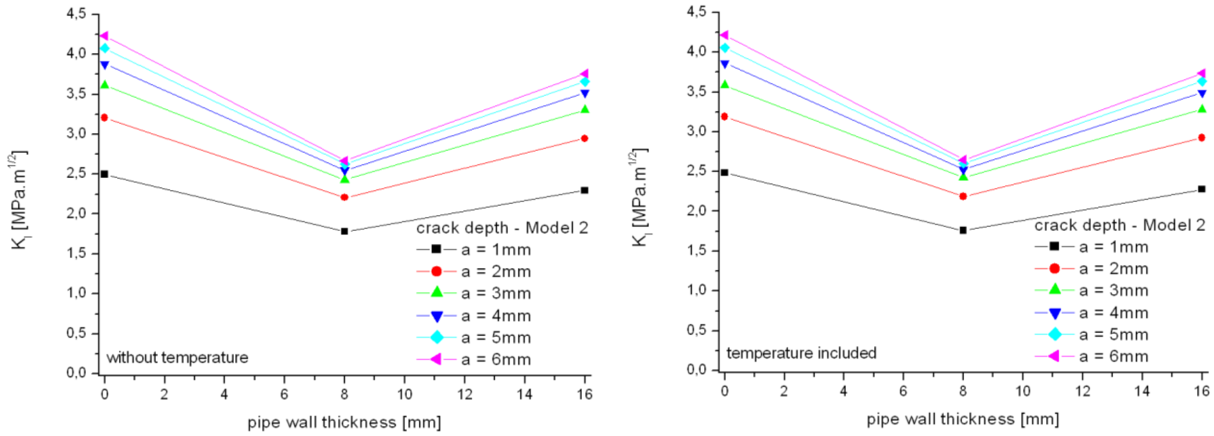

***Fig. 4** Values of K_I factor along the crack front at inner, middle and outer tube radius*
(*0mm corresponds to the outside surface of the tube, 16mm corresponds to the inside surface of the tube*)

Fig. 5 shows distribution of *J*-values along the crack front. Only selected results obtained by contours in circular pattern of the mesh (contour 1, 3 and 7 only) are presented. The advantage gained from calculating the *J*-integral is the use of regular finite elements instead of singular elements necessary for determining of *K*-factors.

Model 1

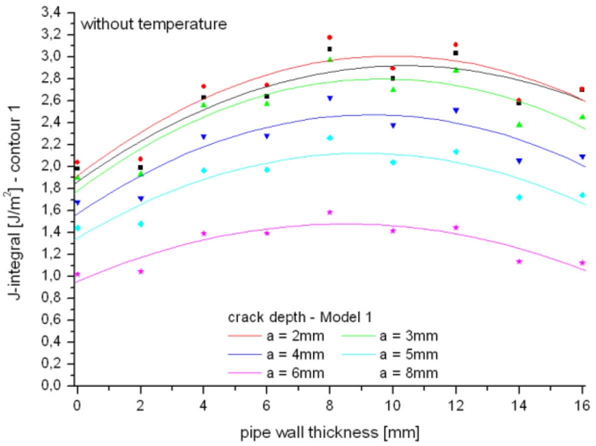

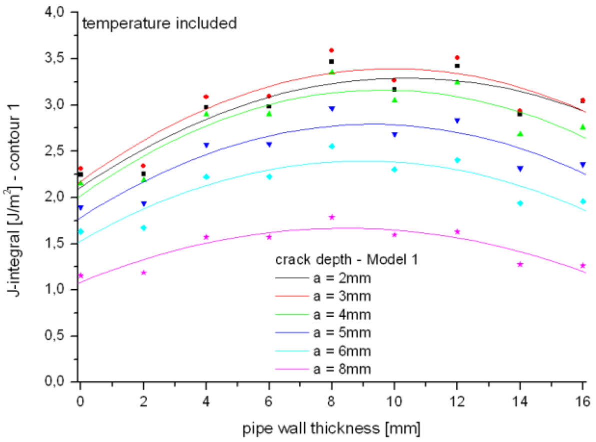

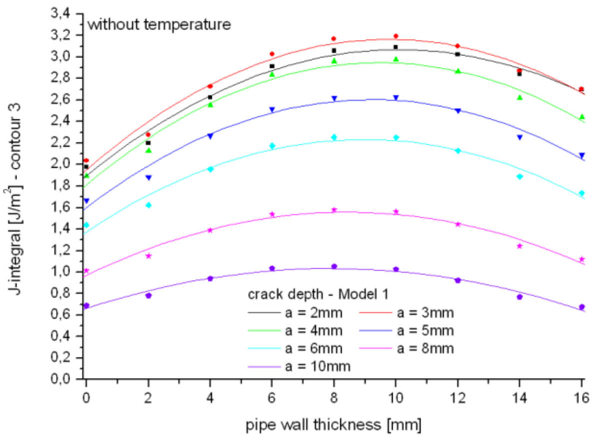

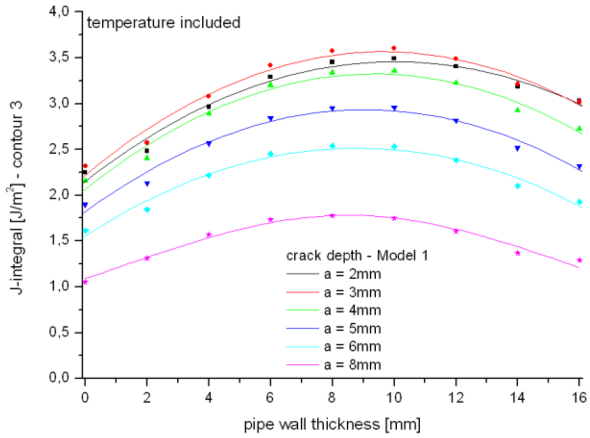

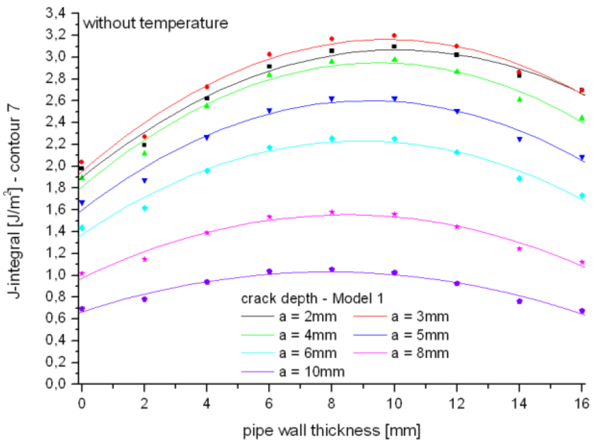

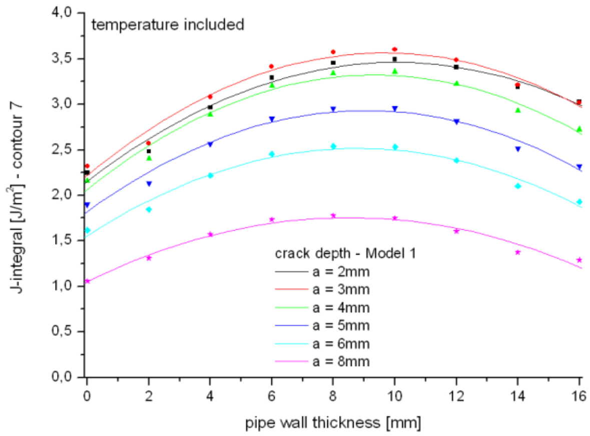

Model 2

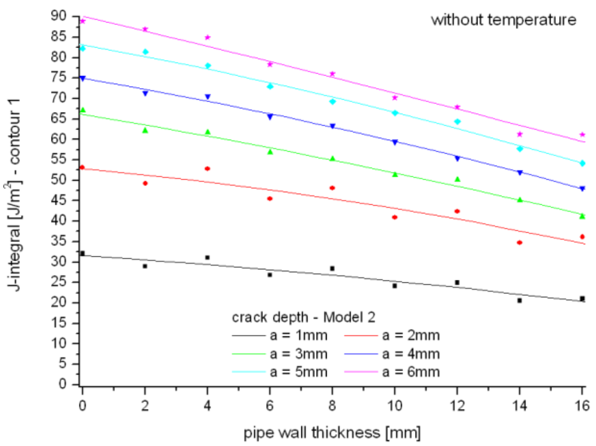

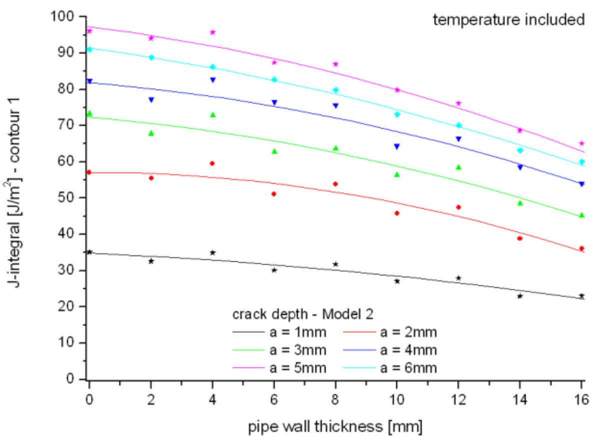

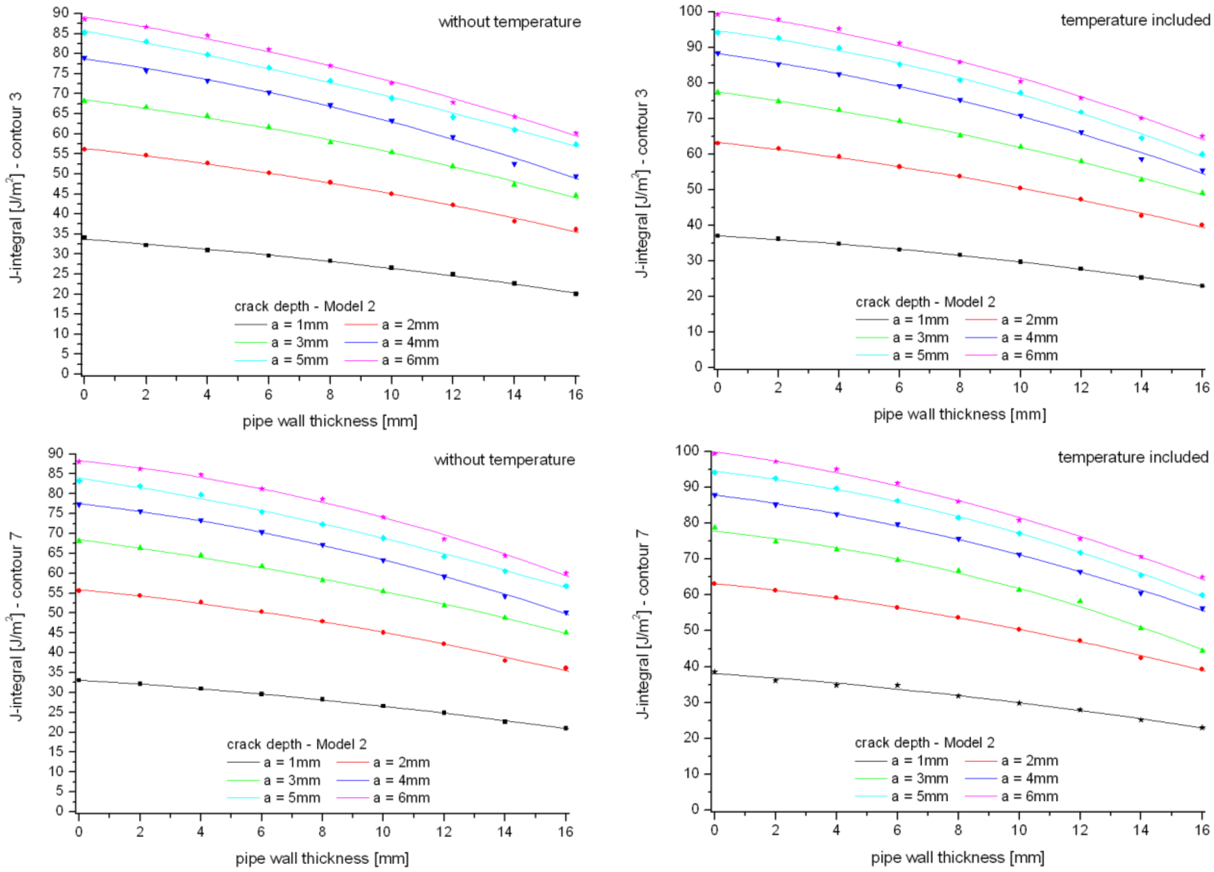

***Fig. 5** J-values along the the crack front for different crack lengths*

Generally it can be concluded that the increase in temperature causes an increase in the value of *J*-integral. Maximum values of *J*-integral along the crack front length (thickness) in *Model 1* were obtained on near middle of the tube wall thickness, however, for *Model 2* maximum values of *J*-integral were localized on the outer surface of the tube.

Fig. 6 shows the dependence of the maximum value of equivalent stress σ_{eqv} in crack front on the crack length *a* for both models with and without considering the effect of temperature field. The value of maximum equivalent stresses are, contrary to expectations, lower when considering the impact of temperature field than in the case without the effect of temperature. This decrease is approximately 1,5% and is caused by change of the elastic modulus with temperature.

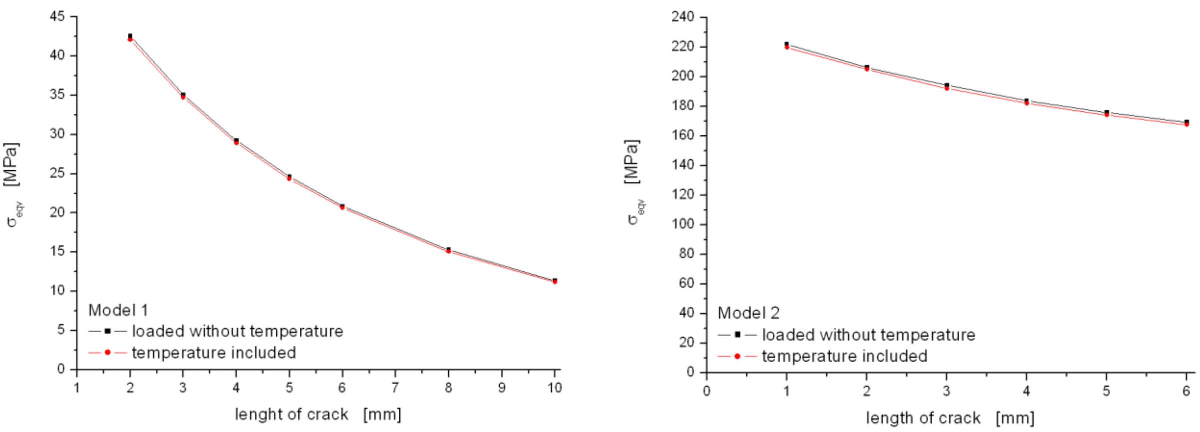

***Fig. 6** Maximum values of equivalent stress σ_{eqv} in the crack front for different crack lengths*

In Fig. 7 the typical distribution of principal stresses σ_1, σ_2 and σ_3 and equivalent (Mises) stress σ_{eqv} near the crack front for selected cases is presented.

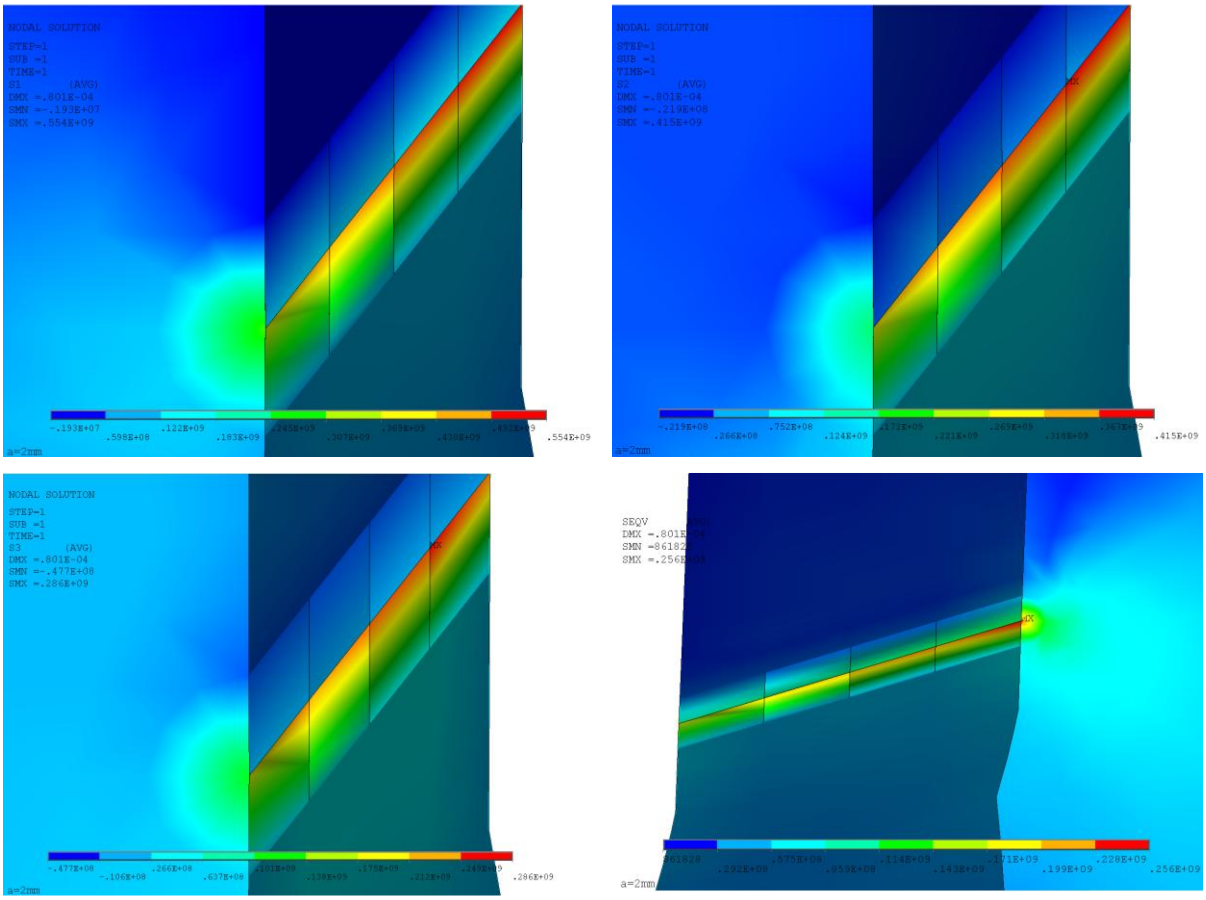

Fig. 7 *Typical stress (principal and equivalent stresses) distribution around crack front (sectional view - Model 2, a = 2mm, temperature field included)*

Conclusion

The paper presents the results of determining the two fracture parameters (SIFs, *J*-integral) used to assess the stability of 3-D crack. Results of *K*-factors strongly depend on element size in the crack front vicinity. Unlike the approach which employs singular quarter mid-nodes and uses the crack tip (front) displacement field to calculate the stress intensity factors, the ANSYS CINT macro is very mesh density sensitive, but the stability is superior. Numerical investigation of the *J*-integral have shown that the near field contour integral loses its path independency, every other fits the *J* better. Out of structured mesh with circular pattern (when contour order exceeds a pattern division), a divergence appears. The results calculated using CINT are almost independent of mesh pattern diameter and of number of divisions as well as of size of element outside.

Under complex loading, presented 3-D fracture analysis gives representative information on the defect behavior. The numerical analysis allows to determine accurately the proces of fracture and consequently to improve the safety of power equipment.

References:

1. BARSOM, J.M., ROLFE, S.T. 1987. Fracture andfatigue control in structures application of fracture mechanics. 2nd. ed. Englewood Cliffs, New York, Prentice Hall.

2. TADA, H., PARIS, P.C., IRWIN, G.R. 1973. *The stress analysis of cracks handbook*. 2nd. ed. St.Louis, Paris.
3. NEWMAN, J.C., RAJU, I.C. 1980. Stress intensity factors for internal surface cracks in cyllindrical pressure vessels. *Trans. J. Pressure Vessel Technology,* ASME, 102.
4. RICE, J.R. 1968. A path independent integral and the approximate analysis of strain concentration by notches and cracks. *J. Appl. Mech*., 35, 379-386.
5. CHIARELLI, M., FREDIANI, A. 1993. A computation of the three-dimensional J-integral for elastic materials with a view to applications in fracture mechanics. *Eng. Frac. Mech,* 44, 763-788.
6. OMER, N., YOSIBASH, Z. 2005. On the path independency of the point-wise J integral in three-dimensions. *Int. J. of Fracture,* 136, 1-36.
7. ANSYS Theory manual, release 14.5.7, 2013.

Reviewers:

prof. Ing. Ladislav Gulan, PhD. – Institute of Transport Technology and Engineering Design, Faculty of Mechanical Engineering STU in Bratislava

doc. Ing. Ľubomír Čaplovič, PhD. – Institute of Materials Science, Faculty of Materials Science and Technology STU in Trnava

Acknowledgement

This publication is the result of implementation of the project: "Increase of Power Safety of the Slovak Republic" (ITMS: 262220220077) supported by the Research & Development Operational Programme funded by the ERDF

Európska únia

Európsky fond regionálneho rozvoja

Operačný program VÝSKUM a VÝVOJ

We support research activities in Slovakia. The project is co-financed by the EU.